Coalesced bainite by isothermal transformation of reheated weld metal

J. H. Pak[1], H. K. D. H. Bhadeshia*[1,2], L. Karlsson[3] and E. Keehan[3,4]

The martensite start and bainite start temperatures have been determined in reheated, high strength weld deposits, with each result associated with 95% coincidence limits. This helped define isothermal transformation temperatures where bainite can be obtained without the risk of unintentional transformation to martensite. It has been demonstrated, therefore, that coalesced bainite, which is detrimental to mechanical properties, can be generated isothermally without the possibility of confusion with autotempered martensite.

Keywords: Coalesced bainite, Phase transformation, Welding, Martensite, Bainite

Introduction

There is tendency to form coarse and hence detrimental plates of bainite in weld metals which transform at large driving forces and relatively low transformation temperatures.[1–7] Such microstructures have also been observed in wrought steels,[8–10] but their presence in weld metals leads to a pronounced reduction in toughness.

The plates, referred to as coalesced bainite, evolve by the coalescence of finer platelets, each of which is separately nucleated but in the same crystallographic orientation during prolonged growth. This leads to a markedly bimodal distribution of plate thicknesses, with the fine plates $\sim 0 \cdot 2$ μm thick and the larger plates many micrometers thick, in three-dimensions.[11] Typical micrographs are presented in Fig. 1. The plate contains cementite particles and it is particularly noticeable that there is a precipitate free zone at its borders. This is because only the carbon near the interface with the austenite can partition once coalescence begins, whereas that remote from the interface must precipitate; this could therefore be regarded as lower bainite.

Although it is commonly believed that lower bainite should contain just one crystallographic variant of cementite,[12–15] it is now established that one or more variants can precipitate in both lower bainite and tempered martensite.[16,17] The question then arises whether the microstructure observed in Fig. 1 really corresponds to bainite or to autotempered martensite. There are indications that the phase forms above the martensite start temperature M_s,[18] but it is difficult to prove this in continuously cooled microstructures.

The purpose of the present work was to establish the bainite start B_s and martensite start temperatures in two weld metals which have previously been studied, and then to see whether coalesced bainite can be generated by isothermal transformation of reheated weld metal above the M_s temperature. This work would therefore help remove the possibility of misinterpreting autotempered martensite as coalesced bainite, and hence contribute to the understanding of a phase which is known to be detrimental to the toughness of strong welds.
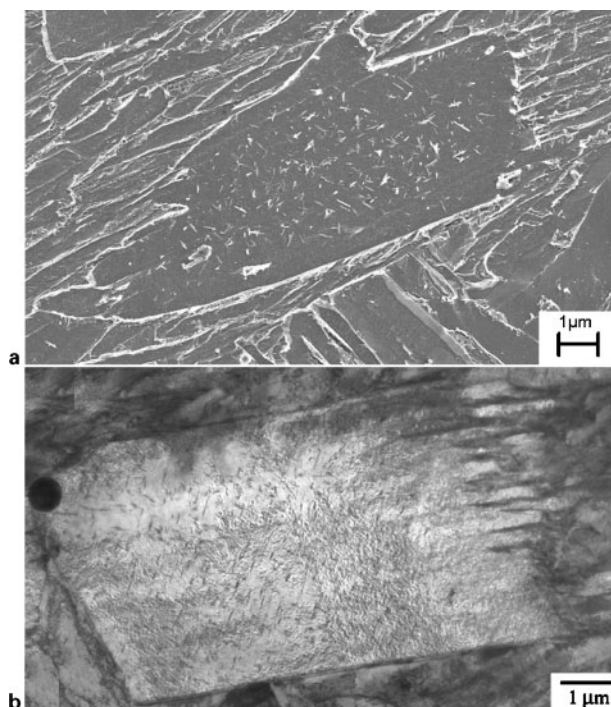

a field emission gun scanning electron micrograph; b transmission electron micrograph
1 Typical micrographs of coalesced bainite in weld metal of composition Fe–0·032C–0·25Si–2·02Mn–7·23Ni–0·47Mn–0·63Mo (wt-%)[3]

[1]Graduate Institute of Ferrous Technology, POSTECH, Pohang, Korea
[2]University of Cambridge, Materials Science and Metallurgy, Cambridge, UK
[3]ESAB AB, Central Research Laboratories, Göteorg, Sweden
[4]Creganna Medical Devices, Creganna, Galway, Ireland

*Corresponding author, email hkdb@postech.ac.kr

(a)

(b)
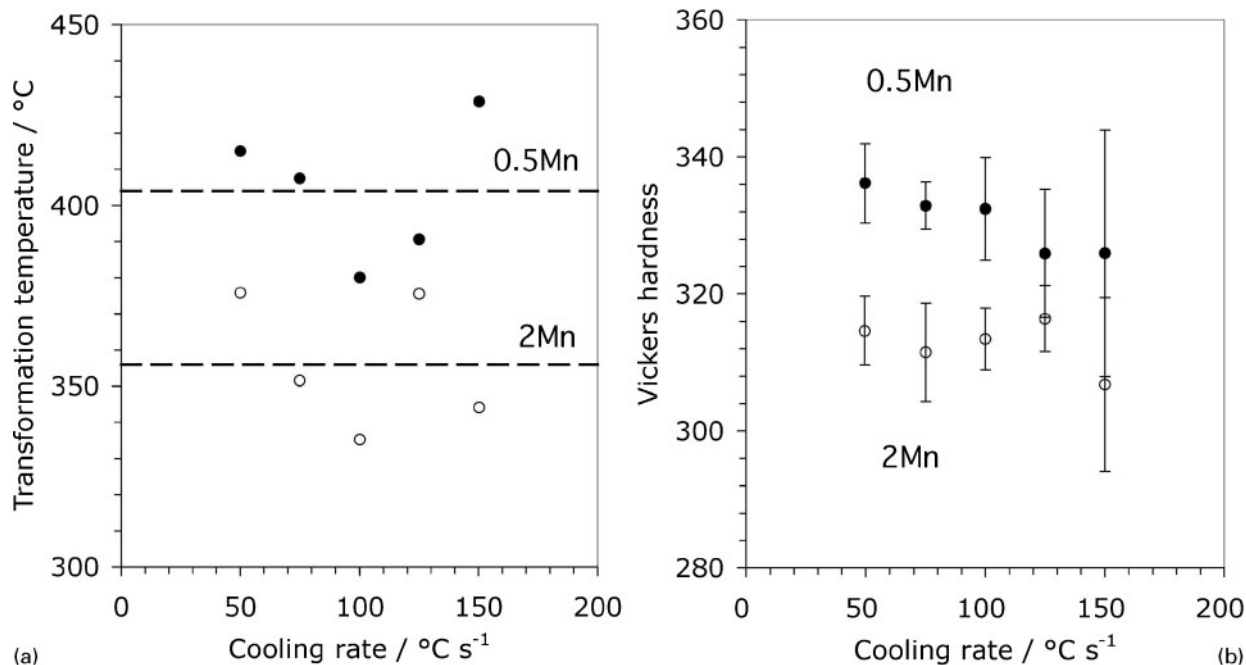
2 *a* transformation temperatures as function of cooling rate and *b* hardness as function of cooling rate

Experimental method

The weld metals used are listed in Table 1 and originate from previous work.[2,19] They are designated as 2Mn and 0·5Mn to indicate the primary difference; the former has been established to show a much greater tendency to form coalesced bainite and hence has poor toughness when compared with the 0·5Mn alloy.[1-7] The welds were produced using the SMAW process, in accordance with ISO 2560 using buttered 20 mm plates and backing plate; this specific joint geometry avoids dilution effects so that the weld metal can be examined in isolation. Each weld consisted of three runs per layer with 22–24 beads per joint. The interpass temperature was 250°C and the heat inputs 1·2 and 1 kJ mm^{-1} for the 2Mn and 0·5Mn welds respectively.

Cylindrical dilatometric samples of diameter 3 mm and length 10 mm were machined with their longitudinal

Table 1 Chemical compositions of two weld metals (i.e. weld deposit) designated as 2Mn and 0·5Mn, wt-%

Alloy	C	Si	Mn	P	S	Cr	Ni	Mo	W
2Mn	0·03	0·23	2·05	0·01	0·008	0·43	7·1	0·63	0·004
0·5Mn	0·025	0·39	0·58	0·01	0·009	0·15	6·5	0·39	0·001
	Co	V	Nb	Cu	Al	Ti	B	O	N
2Mn	0·008	0·021	0·004	0·02	0·001	0·011	0·0012	0·031	0·011
0·5Mn	0·009	0·018	0·002	0·02	0·001	0·015	0·0012	0·033	0·009

Table 2 Measured martensite start temperatures and $\pm 1\sigma$ standard error associated with each measurement

T, °C s^{-1}	0·5Mn M_s, °C	2Mn M_s, °C
150	429±0·6	344±0·1
125	391±0·6	376±0·6
100	380±0·6	335±2·1
75	408±1·3	351±0·2
50	414±4·0	376±0·6

(a)

(b)

(c)
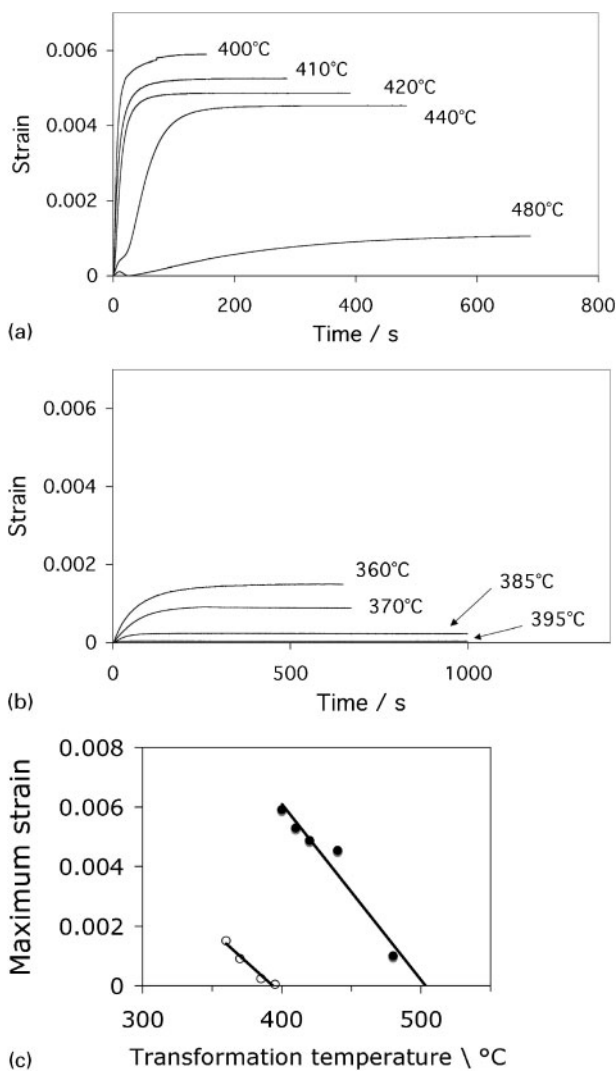
a 0·5Mn; *b* 2Mn; *c* extrapolation, using linear regression, of maximum strain observed at any transformation temperature, to determine B_s temperature

3 Dilatometric data showing isothermal transformation to bainite
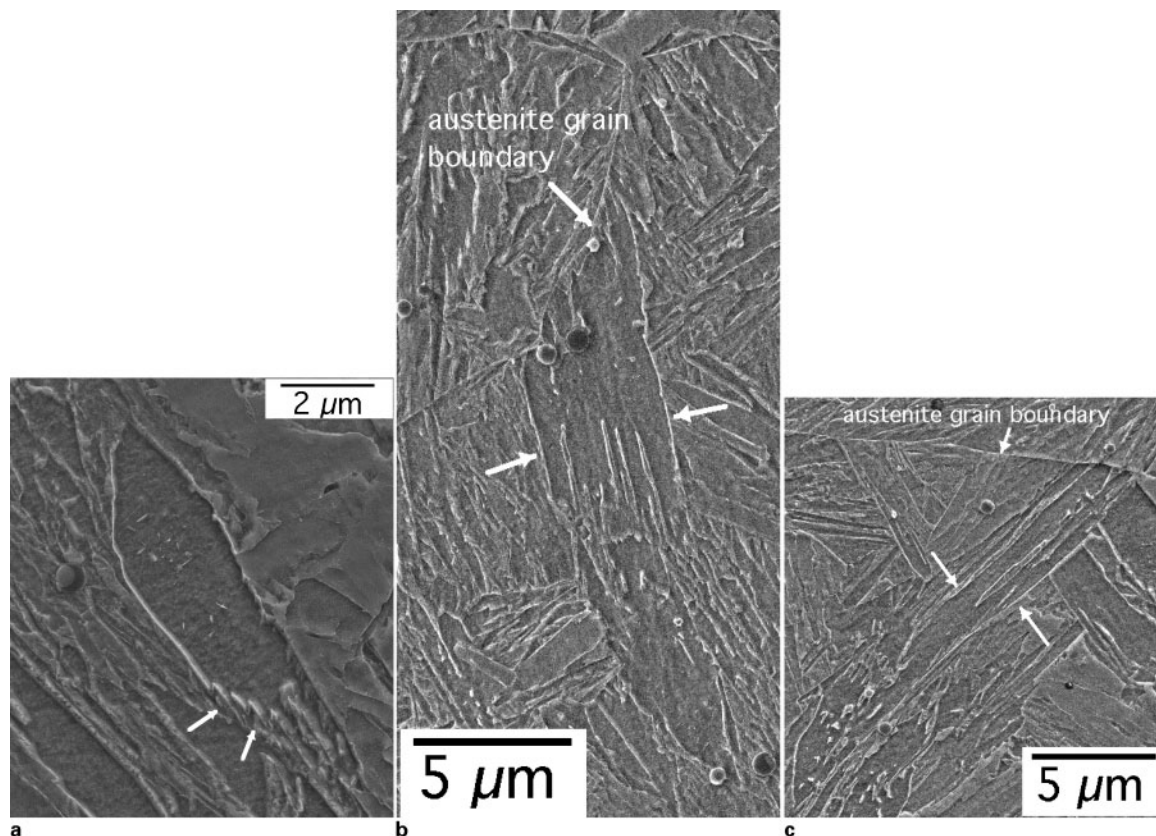
a edges of platelets contributing to coalescence process; *b* coalescence occurring at leading edges of platelets nucleated at common austenite boundary; *c* coalescence only possible with extended growth

4 Micrographs showing coalesced bainite in 2Mn alloy heat treated at 385°C for 3 h: unmarked arrows show regions where coalescence process has been captured; some particles of cementite are evident within coarse plate in *a*

directions parallel to the welding direction so that they only consisted of weld metal. A push rod BAHR DIL805 high speed dilatometer with radio frequency induction heating was used. The sample temperature is measured by a thermocouple welded to its surface using a precision welder and jig supplied by the dilatometer manufacturer.

Each sample for the M_s temperature determination was austenitised at 1100°C for 3 min, followed by helium quenching at a variety of constant cooling rates. For isothermal transformation following austenitisation, the samples were quenched to the isothermal transformation temperature within 7 s following austenitisation at 1100°C for 5 min. The austenitisation times of 3 and 5 min led to austenite grain sizes (measured using the lineal intercept method) of 60 ± 6 and 72 ± 8 μm respectively. This should only affect the strength of the austenite by ~ 1 MPa[20] and hence the martensite start temperature by less than 1°C.[21]

Each heat treated sample was used once and retained for standard metallographic and Vickers hardness tests.

Transformation temperatures

In recent work,[22] the authors have defined a method for the objective interpretation of dilatometer data; with this offset method, an independent assessment of the data should lead to the same transformation temperature. The transformation start temperature is that at which the plot of strain versus temperature deviates from thermal contraction by a specified amount. The latter quantity corresponds to strain involved in the formation

of 1% of martensite at 25°C as determined from the calculated lattice parameters of the austenite and martensite.[22] Note that the accuracy of the calculation of lattice parameter is not relevant: the important point in the offset method is to state the strain at which the M_s is measured, so that another investigator using the same data can reach an exactly identical transformation temperature.[22]

The results from dilatometric experiments designed to measure the martensite start temperature are plotted in Fig. 2*a*, from which the M_s temperatures are determined to be 356 ± 21 and 404 ± 21°C for the 2Mn and 0·5Mn alloys respectively, where the stated uncertainty is simply the standard deviation about the mean of all the values measured. The scatter observed in Fig. 2*a* is real in that the error associated with the interpretation of the precision dilatometric data is, for all the experiments, less than ± 4°C. The scatter is inconsistent with the detailed analysis of transformation temperatures presented in[22] and with published neural network analysis of large quantities of similar data.[23,24]

It is important to note that on the basis of the maximum values listed in Table 2, the upper limits to the M_s temperatures, with 95% confidence limits, are 430·2 and 377·2°C for the 0·5Mn and 2Mn alloys respectively. Therefore, the isothermal transformation experiments reported later are performed at temperatures above these values in order to ensure reaction within the bainite transformation temperature range.

The reasons for expecting such levels of scatter have been discussed in detail[22] and are not repeated here.
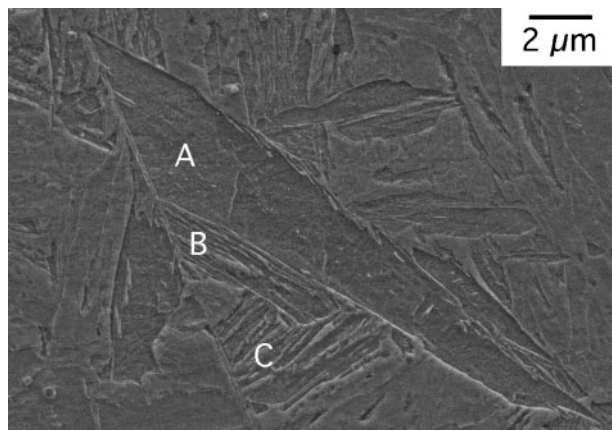
5 Micrograph of 2Mn alloy transformed isothermally at 395°C for 7 h: there are three marked regions, all originating at austenite grain boundary; 'A' is large plate of coalesced bainite; 'B' and 'C' show ordinary, fine plates of bainite

However, it is pertinent to note that the hardness data (Fig. 2*b*) are consistent with martensite being obtained for all cooling rates in the range 50–150°C s^{-1}.

The method for measuring the bainite start temperature exploited the incomplete reaction phenomenon.[13,14,25–30] In this phenomenon, the extent of reaction tends towards zero as the transformation temperature is increased towards B_s. This is because the driving force for either the diffusionless growth or the nucleation of bainite is exhausted at the B_s temperature.[31] The effect is prominent in steels where cementite precipitation is retarded relative to the formation of bainitic ferrite, either by the judicious use of solutes such as Si or Al, or when the steel contains a carbon concentration which is so small that the kinetics of cementite formation are slow.[32,33]

Figure 3 shows isothermal transformation dilatometric curves for the two alloys studied here: it is evident that in both cases, the dilatation due to transformation tends to diminish as the transformation temperature is increased. On extrapolating the observed maximum extent of transformation to zero, the B_s temperatures were determined to be 393 ± 11 and 503 ± 34°C for the 2Mn and 0·5Mn alloys respectively.

Metallography

The purpose of the metallography was primarily to demonstrate that coalesced bainite can be obtained at temperatures above that at which martensite forms, even when taking account of the uncertainties in the measurement of the M_s temperature. Figure 4 illustrates a sample of the 2Mn alloy transformed isothermally at 385°C for 3 h, bearing in mind that the upper limit of the M_s temperature to 95% confidence limits is 377°C. There seems to be clear evidence for the coalesced bainite.

Figure 5 shows coalesced bainite (marked as 'A'), originating at an austenite grain boundary, in a 2Mn alloy transformed isothermally at the even higher temperature of 395°C. Of particular interest are the two colonies of fine platelets of bainite (marked as 'B' and 'C'), also initiating from the austenite grain boundary. Neither of these have developed into coarse
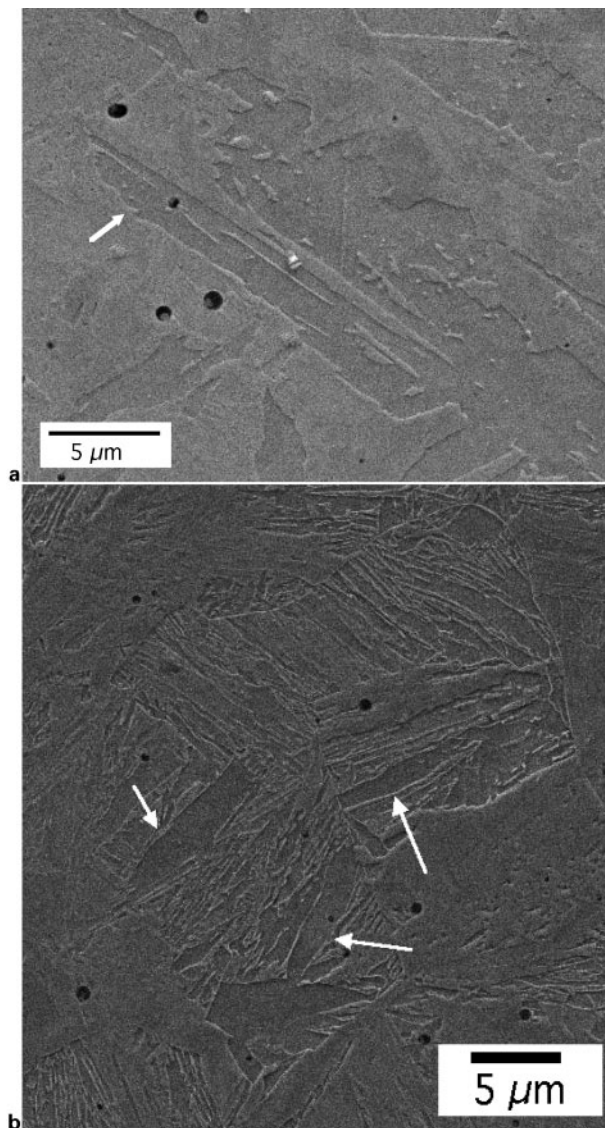
6 Micrographs showing coalesced bainite in 0·5Mn alloy isothermally transformed at *a* 440 and *b* 480°C: note discontinuous films of residual phase between within coalesced bainite (arrowed), indicative of merging of subunits; *b* 480°C showing several coalesced plates with finer bainite in between

bainite, because as hypothesised some time ago, the coalescence process need space to evolve:[7,10] these two colonies have been stifled in their development by impingement with each other and with the coalesced plate.

Similar experiments were carried out for the 0·5Mn alloy, i.e. isothermal transformation at 440 and 480°C, above the upper limit of the M_s temperature to 95% confidence limits at 430°C. The results, illustrated in Fig. 6, show the presence of coalesced bainite interspersed with the finer platelets.

Conclusion

The fact that coalesced bainite has been obtained by isothermal transformation in reheated weld deposits, under conditions where martensite is not expected, shows that the phase cannot be confused with auto-tempered martensite. The metallography coincidentally

illustrates the process of coalescence and the coexistence of fine and coarse bainite plates in an apparently bimodal distribution.

Acknowledgement

References

1. E. Keehan, L. Karlsson, M. Marimuthu, H.-O. Andrén and H. K. D. H. Bhadeshia: in 'Today and tomorrow in the science and technology of welding and joining' (ed. T. Ohji), 797–802; 2001, Tokyo, Japan Welding Society.
2. E. Keehan, H.-O. Andrén, L. Karlsson, M. Murugananth and H. K. D. H. Bhadeshia: in 'Trends in welding research' (ed. S. A. David and T. DebRoy), 695–700; 2002, Materials Park, OH, ASM International.
3. E. Keehan, L. Karlsson and H.-O. Andrén: *Sci. Technol. Weld. J.*, 2006, **11**, 1–8.
4. E. Keehan, L. Karlsson, H.-O. Andrén and H. K. D. H. Bhadeshia: *Sci. Technol. Weld. Join.*, 2006, **11**, 9–18.
5. E. Keehan, L. Karlsson, H.-O. Andrén and H. K. D. H. Bhadeshia: *Sci. Technol. Weld. Join.*, 2006, **11**, 19–24.
6. E. Keehan, L. Karlsson, H.-O. Andrén and L.-E. Svensson: *Weld. J.*, 2006, **85**, 211s–218s.
7. H. K. D. H. Bhadeshia, E. Keehan, L. Karlsson and H. O. Andrén: *Trans. Ind. Inst. Met.*, 2006, **59**, 689–694.
8. H. K. D. H. Bhadeshia and D. V. Edmonds: *Metall. Trans. A*, 1979, **10A**, 895–907.
9. R. Padmanabhan and W. E. Wood: *Mater. Sci. Eng.*, 1984, **66**, 1–11.
10. L. C. Chang and H. K. D. H. Bhadeshia: *Mater. Sci. Technol.*, 1996, **12**, 233–236.
11. E. Keehan, L. Karlsson, H. K. D. H. Bhadeshia and M. Thuvander: *Mater. Character.*, 2008, **59**, 877–882.
12. G. R. Srinivasan and C. M. Wayman: *Acta Metall.*, 1968, **16**, 621–636.
13. R. F. Hehemann: in 'Phase transformations' (ed. H. I. Aaronson and V. F. Zackay), 397–432; 1970, Materials Park, OH, ASM International.
14. R. F. Hehemann, K. R. Kinsman and H. I. Aaronson: *Metall. Trans.*, 1972, **3**, 1077–1094.
15. G. R. Srinivasan and C. M. Wayman: *Acta Metall.*, 1968, **16**, 609–620.
16. H. K. D. H. Bhadeshia: *Acta Metall.*, 1980, **28**, 1103–1114.
17. J. W. Stewart, R. C. Thomson and H. K. D. H. Bhadeshia: *J. Mater. Sci.*, 1994, **29**, 6079–6084.
18. E. Keehan: 'Effect of microstructure on mechanical properties of high-strength steel weld metals', PhD thesis, Chalmers University, Göteborg, Sweden, 2005.
19. M. Murugananth, H. K. D. H. Bhadeshia, E. Keehan, H. O. Andren and L. Karlsson: in 'Mathematical modelling of weld phenomena 6' (ed. H. Cerjak and H. K. D. H. Bhadeshia), 205–230; 2002, London, Maney.
20. B. P. Kashyap and K. Tangri: *Scr. Metall. Mater.*, 1990, **24**, 1777–1782.
21. P. J. Brofman and G. S. Ansell: *Metall. Trans. A*, 1983, **14A**, 1929–1931.
22. H.-S. Yang and H. K. D. H. Bhadeshia: *Mater. Sci. Technol.*, 2007, **23**, 556–560.
23. J. Wang, P. J. van der Wolk and S. van der Zwaag: *Mater. Trans. JIM*, 2002, **41**, 761–768.
24. W. G. Vermeulen, P. F. Morris and S. van der Zwaag: *Ironmaking Steelmaking*, 1996, **23**, 433–437.
25. V. S. Steinberg and V. Susin: *Arch Eisenhuttenw.*, 1934, **9**, 537–538.
26. R. Le-Houillier, G. Begin and A. Dube: *Metall. Trans.*, 1971, **2**, 2645–2653.
27. H. K. D. H. Bhadeshia and D. V. Edmonds: *Acta Metall.*, 1980, **28**, 1265–1273.
28. P. G. Self, H. K. D. H. Bhadeshia and W. M. Stobbs: *Ultramicroscopy*, 1981, **6**, 29–40.
29. M. Takahashi and H. K. D. H. Bhadeshia: *Mater. Trans. JIM*, 1991, **32**, 689–696.
30. T. Lyman and A. R. Troiano: *Trans. ASM*, 1946, **37**, 402–448.
31. H. K. D. H. Bhadeshia: *Acta Metall.*, 1981, **29**, 1117–1130.
32. H. K. D. H. Bhadeshia: 'Bainite in steels', 2nd edn; 2001, London, Institute of Materials.
33. H.-S. Yang and H. K. D. H. Bhadeshia: *Mater. Sci. Technol.*, 2008, **24**, 335–342.